Quasiparticle statistics and braiding from ground-state entanglement

Yi Zhang, Tarun Grover, Ari Turner, Masaki Oshikawa, and Ashvin Vishwanath

Phys. Rev. B **85**, 235151 — Published 29 June 2012

DOI: 10.1103/PhysRevB.85.235151

Quasi-particle Statistics and Braiding from Ground State Entanglement

Yi Zhang,[1] Tarun Grover,[1] Ari Turner,[2] Masaki Oshikawa,[3] and Ashvin Vishwanath[1]

[1]*Department of Physics, University of California, Berkeley, CA 94720, USA*
[2]*University of Amsterdam, Science Park 904, P.O.Box 94485, 1090 GL Amsterdam, The Netherlands*
[3]*Institute for Solid State Physics, University of Tokyo, Kashiwa 277-8581, Japan*

Topologically ordered phases are gapped states, defined by the properties of excitations when taken around one another. Here we demonstrate a method to extract the statistics and braiding of excitations, given just the set of ground-state wave functions on a torus. This is achieved by studying the Topological Entanglement Entropy (TEE) on partitioning the torus into two cylinders. In this setting, general considerations dictate that the TEE generally differs from that in trivial partitions and depends on the chosen ground state. Central to our scheme is the identification of ground states with minimum entanglement entropy, which reflect the quasi-particle excitations of the topological phase. The transformation of these states allows for a determination of the modular $\mathcal{S}$ and $\mathcal{U}$ matrices which encode quasi-particle properties. We demonstrate our method by extracting the modular $\mathcal{S}$ matrix of a chiral spin liquid phase using a Monte Carlo scheme to calculate TEE, and prove that the quasi-particles obey semionic statistics. This method offers a route to a nearly complete determination of the topological order in certain cases.

PACS numbers:

I. INTRODUCTION

Topologically ordered states are gapped quantum phases of matter that lie beyond the Landau symmetry breaking paradigm [1]. Well known examples include fractional quantum Hall states and gapped quantum spin liquids [1–10]. These phases are not characterized by local correlations or order parameters but rather by long range entanglement in their ground-state wave functions [11]. Recently, there has been renewed interest in such states, both from a fundamental perspective, as well as with a view to applications in quantum computing[12]. At the fundamental level, topologically ordered phases display a number of unique properties. In two dimensions, emergent excitations in these states display nontrivial statistics. In Abelian topological phases, exchange of identical excitations or taking one excitation around another (braiding) leads to characteristic phase factors, that are neither bosonic nor fermionic. A further remarkable generalization of statistics occurs in non-Abelian phases where excitations introduce a degeneracy. Braiding excitations then leads to a unitary transformation on these degenerate states, which generalizes the phase factor of Abelian states.

These striking properties of topologically ordered phases are connected to excitations. An important and interesting question is whether the ground state directly encodes this information, and if so how one may access it. It is well known that topologically ordered phases feature a ground state degeneracy that depends on the topology of the space on which they are defined. Also, ground states of such states contain a topological contribution to the quantum entanglement, the topological entanglement entropy (TEE) [13–15]. In this paper we show that combined together, these two ground state properties can be used to extract the generalized statistics associated with excitations in these states. We apply these insights to a chiral spin-liquid wavefunction, and numerically extract the semionic statistics associated with excitations. This demonstrates the promise of this approach in helping numerical studies diagnose the precise character of topological order in a particular state.

The generalized statistics of quasiparticles is formally captured by the modular $\mathcal{S}$ and $\mathcal{U}$ matrices, in both Abelian and non-Abelian states [3, 12, 16–18]. The element $\mathcal{S}_{ij}$ of the modular $\mathcal{S}$ matrix determines the mutual statistics of i'th quasiparticle with respect to the j'th quasiparticle while the element $\mathcal{U}_{ii}$ of (diagonal) $\mathcal{U}$ matrix determines the self-statistics ('topological spin') of the i'th quasiparticle. Note, these provide a nearly complete description of a topologically ordered phase - for instance, fusion rules that dictate the outcome of bringing together a pair of quasiparticles, are determined from the modular $\mathcal{S}$ matrix, by the Verlinde formula[19]. Previously, Wen proposed [3] using the non-Abelian Berry phase to extract statistics of quasiparticles. However, the idea in Ref. [3] requires one to have access to an *infinite set of ground-states* labeled by a continuous parameter, and is difficult to implement. Recently, Bais et al. [20] also discussed extracting $\mathcal{S}$ matrix in numerical simulations, by explicit braiding of excitations. In contrast, here we will just use the set of ground states on a torus, to determine the braiding and fusing of gapped excitations.

Recall, the ground-state entanglement entropy of a two dimensional topologically ordered phase in a disk-shaped region A with a smooth boundary of length L takes the form $S_A = \alpha L - \gamma$, where the universal constant γ is the TEE [13–15]. The constant γ equals $\log(D)$ where $D = \sqrt{\sum d_i^2}$ is the "total quantum dimension" associated with the topological phase while d_i is the quantum dimension of i'th quasiparticle type. For Abelian states $d_i = 1$ so D^2 is simply the number of quasiparticle types in the theory. This is also the ground state degeneracy

on a torus. For example, the simplest case of $D^2 = 2$ corresponds to the chiral spin liquid or equivalently the $\nu = 1/2$ bosonic Laughlin state[21]. This has, in addition to the trivial excitation, a semionic quasiparticle. Unfortunately, the total quantum dimension D only provides a partial characterization of topological order since two distinct topological phases can have same value of D. For example, the topological phase based on a Z_2 gauge theory has $D^2 = 4$, which could also be achieved with two decoupled copies of the chiral spin liquid. However a knowledge of the modular $\mathcal{S}$ matrix could tell these states apart.

It is sometimes stated without qualification, that TEE is a quantity solely determined by the total quantum dimension D of the underlying topological theory. However, this holds true *only when the boundary of the region A consists of topologically trivial closed loops*. If the boundary of region A is non-contractible, for example if one divides the torus into a pair of cylinders, *generically the entanglement entropy is different for different ground states* (see Figure 1). Indeed as shown in Ref. 22 for a class of topological states, the TEE depends on the particular linear combination of the ground states when the boundary of region A contains non-contractible loops. We will exploit this dependence to extract information about the topological phase beyond the total quantum dimension D.

At a practical level, recent progress in numerical techniques have lead to a number of proposals for topologically ordered spin liquid phases on the Kagome [23, 24], honeycomb [25] and square lattice with diagonal exchange [26, 27]. A number of lattice states related to the Laughlin states have also been proposed in recent numerical studies [28–32]. Clearly, smoking gun numerical signatures of topological order are increasingly needed. The procedure outlined here suggests that entanglement entropy could be used to numerically diagnose details of topological order beyond the total quantum dimension [33–37], which is a single number susceptible to numerical error. An elegant different approach to a more complete identification of topological order is through the study of the entanglement spectrum [38]. However we note that requires the existence of edge states and may not be applicable for topological phases like the Z_2 spin liquid. For concreteness, consider the following problem of identifying a topological phase which is known to have quantum dimension $D = 2$. While Z_2 gauge theories have this quantum dimension, there is another theory, doubled Chiral Spin Liquid[39], which also has the same quantum dimension and is also time reversal symmetric. The S-matrix can tell these apart, since the latter phase contains semions, and we show how S-matrix can, in principle, be extracted from the entanglement entropy. Note, entanglement spectrum cannot tell these phases apart since they do not in general have protected edge states. Furthermore, it is possible to compute TEE using Monte Carlo techniques on relatively larger systems [33, 37], as also done in this paper, where the entanglement spectrum is not currently available.

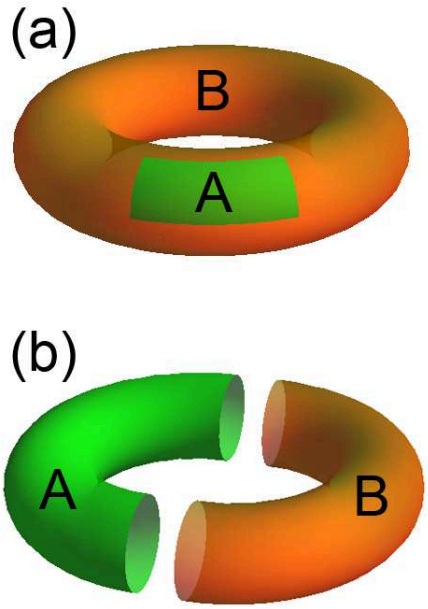

FIG. 1: Two types of entanglement bipartitions on the torus: (a) A trivial bipartition with contractible boundaries for which the TEE $\gamma = \log D$, and (b) A bipartition with non-contractible boundaries, where the TEE depends on ground state.

Let us briefly summarize the key ideas involved in this work. We recall that the number of ground states on a torus corresponds to the number of distinct quasiparticle types. Intuitively, different ground states are generated by inserting appropriate fluxes 'inside' the cycle of the torus, which is only detected by loops circling the torus. We would like to express these quasiparticle states as a linear combination of ground states. A critical insight is that this can be done using the topological entanglement entropy for a region A that wraps around the relevant cycle of the torus. With this in hand one can readily access the modular $\mathcal{S}$ and $\mathcal{U}$ matrices. For example, the $\mathcal{S}$ matrix is obtained by relating quasiparticle states associated with different cycles of the torus.

We begin by elaborating on the ground-state dependence of entanglement entropy, focusing on the case of a partition of torus into two cylinders (Sec.II B). We present an argument based on the strong subadditivity property of quantum information and show that the TEE per connected boundary is not identical to that for a trivial bipartition, such as a disc cut out of the torus. This is illustrated as an 'uncertainty' relation, between entropies for two different cylindrical bipartitions of the torus. We introduce the notion of *minimum entropy states (MESs)*, namely the ground states with minimal entanglement entropy (or maximal TEE, since the TEE always reduces the entropy) for a given bipartition. These states can be identified with the quasi-particles of the topological

phase and generated by insertion of the quasi-particles into the cycle enclosed by region A. For a generic lattice wave function with finite correlation length, such as the Chiral Spin Liquid wave functions we study later, a non-local measurement like TEE is essential to identify this basis of MESs.

In sec.III we detail a procedure that uses the ground state dependence of TEE to extract the key properties of quasi-particle excitations by determining modular $\mathcal{S}$ and $\mathcal{U}$ matrices. The basic idea is to relate MESs for different entanglement bipartitions of the torus. The MESs, which reflect quasi-particle excitations, are determined using TEE.

In Sec.IV A 1 we demonstrate the ground-state dependence numerically, and calculate the entanglement entropy for the chiral spin liquid [21] (CSL) wave function as different linear superpositions of the two ground states (Figure 5) with the Variational Monte Carlo (VMC) method [33, 40, 41]. This directly yields the modular $\mathcal{S}$ matrix of the CSL state which also enables use to detect the presence of a semionic excitation in CSL. The physical origin of the ground-state dependence of TEE is made explicit by studying a Z_2 toric code model [11] (Sec.IV B). For pedagogical purposes, in Appendix E we discuss the extraction of the modular $\mathcal{S}$ and $\mathcal{U}$ matrices for the toric code model using our algorithm.

II. GROUND STATE DEPENDENCE OF TOPOLOGICAL ENTANGLEMENT ENTROPY

A. The Concept of "Minimum Entropy States"

Given a normalized wave function $|\Phi\rangle$ and a partition of the system into subsystems A and B, one can trace out the subsystem B to obtain the reduced density matrix on subsystem A: $\rho_A = Tr_B |\Phi\rangle \langle\Phi|$. The Renyi entropies are defined as:

$$S_n = \frac{1}{1-n} \log \left(Tr \rho_A^n\right)$$

where n is an index parameter. Taking the limit $n \to 1$, S_n recovers the definition of the usual von Neumann entropy. In this paper we will often discuss the Renyi entropy with index $n = 2$: $S_2 = -\log\left(Tr\left(\rho_A^2\right)\right)$ since it can be calculated most easily with the VMC method[33] and at the same time, captures all the information that we are interested in.

For a gapped phase in 2D with topological order and a disc shaped region A with smooth boundary of length L_A, the Area Law of the Renyi entropy gives:

$$S_n = \alpha_n L_A - \gamma \tag{1}$$

where we have omitted the sub-leading terms. Although the coefficient α_n of the leading 'boundary law' term is non-universal, the sub-leading constant γ, which is often dubbed as the TEE, is universal and a robust property of the phase of matter for which $|\Phi\rangle$ is the ground state. When region A has a disc geometry, it has been shown that γ for different degenerate ground states are identical and it is also insensitive to the Renyi entropy index n [22, 42]. It equals $\gamma = \log D$, where D is the total quantum dimension of the model [14, 15], and offers a partial characterization of the underlying topological order.

However, when the subsystem A takes a non-trivial topology, or more precisely when the boundary of A is non-contractible, TEE contains more information [22], as we will elaborate further in this paper. For simplicity of illustration, throughout we focus on the case when the two-dimensional space is a torus T_2 and the subsystem A wraps around the $\hat{y}$ direction of the torus and takes the geometry of a cylinder. For such a geometry, the n'th Renyi entropy corresponding to the wave function $|\Phi\rangle = \sum_j c_j |\Xi_j\rangle$ is given by: $S_n = \alpha_n L_A - \gamma_n'$, where $|\Xi_j\rangle$ is a special basis that we will describe in detail below and γ_n' is given by [22]:

$$\gamma_n'\left(\{p_j\}\right) \;=\; 2\gamma + \frac{1}{n-1} \log\left(\sum_j p_j^n d_j^{2(1-n)}\right) \tag{2}$$

Here $d_j \geq 1$ is the quantum dimension of the jth quasi-particle and $p_j = |c_j|^2$. For Abelian anyons, $d_j = 1$. Note, d_j shares the same subscript j as the states $|\Xi_j\rangle$ because the states $|\Xi_j\rangle$ can be obtained by inserting a quasi-particle with quantum dimension d_j (the ground state degeneracy on the torus is equal to the number of distinct quasi-particles). This equation shows that the TEE for this geometry depends on the wave function through $\{p_j\}$ as well as the Renyi index n, unlike the case with disc geometry.

What is the physical significance of the basis states $|\Xi_j\rangle$? We claim that these are precisely the eigenstates of the nonlocal operators defined on the entanglement cut, which distinguish the topologically degenerate ground states. For example, in the case of the quantum Hall [22] (Sec. IV A 2), these states are the eigenstates of the Wilson loop operator associated with the Chern-Simons gauge field around the hole exposed by the entanglement cut. Similarly, for a Z_2 gauge theory (Sec. IV B), these are the states with definite electric and magnetic field fluxes perpendicular to the entanglement cut. For Abelian states, which have $d_j = 1$ for all j and are the focus of this paper, the entanglement entropy associated with the states $|\Xi_j\rangle$ is minimum, i.e. heuristically, the entanglement cut has the maximum 'knowledge' about these states. For this reason we name them *Minimum Entropy States (MESs).*

B. Strong Subadditivity and Topological Entanglement Entropy on the Torus: An 'uncertainty' principle

In this section we discuss the TEE for bipartitions of a torus into two cylinders. This can be done by slicing the torus in two distinct ways, along the vertical or horizontal directions. Intuitively, one might expect both bipartitions would have the same TEE of 2γ, given the two disconnected boundaries of the cylinders. However, very general considerations based on strong subadditivity of von-Neumann entropy alone suggest that this expectation cannot be correct. In practice, it is known that for a wide class of topological phases, TEE of such non-trivial bipartitions indeed depends on the ground state selected[22]. Here we do not address ground-state dependence, rather we demonstrate that TEE cannot be identical to its value for trivial bipartitions. It invokes strong subadditivity, a deep property of quantum information [43]. This will allow us to come up with an uncertainty principle, which constrains the amount of information we have when we cut the torus in two orthogonal directions. Its advantage is that it assumes almost nothing about the phase, except that it is gapped.

Consider the ground-state wave function of a gapped phase in two dimensions and three non-overlapping subregions A, B, C. The von-Neumann entropies S follow the strong subadditivity condition[43]:

$$S_{ABC} + S_B - S_{AB} - S_{BC} \leq 0 \tag{3}$$

Note, this is only known to hold for von-Neumann entropies, not Renyi entropies in general. Now, consider a torus with subregions A, B, C as shown in the Fig. 2. Let us decompose the entropy into a part that arises from local contributions and a non-local TEE $S = S^{\text{local}} + S^{\text{topo}}$. For a subregion with the topology of a disc, the TEE is expected to be $S^{\text{topo}} = -\gamma$. Quite generally one can argue that $\gamma \geq 0$ utilizing the strong subadditivity condition [14]. For subregions defined on a simply connected surface, such as a disc, the TEE is proportional to the number of connected components of the boundary. If this was also true for the torus, we would expect $S^{\text{topo}}_{AB} = S^{\text{topo}}_{BC} = -2\gamma$ (since they have a a pair of boundaries). We now show this cannot be a consistent assignment of TEE on the torus.

In order to isolate the topological part of the entropy, we assume that the regions A and C are well separated compared to the correlation length of the gapped ground state. Then, the local contributions cancel in the combination above: $S^{\text{local}}_{ABC} + S^{\text{local}}_{B} - S^{\text{local}}_{AB} - S^{\text{local}}_{BC} \to 0$. This can be argued following Refs.[14, 15]. For example, consider a local deformation near region A's boundary far away from the other regions. This change will be in S^{local}_{ABC}, but a nearly identical contribution will also appear in S^{local}_{AB}, since it only differs by the addition of a distant region. These will cancel in the combination above. Thus, we can rewrite the Eqn. 3 as:

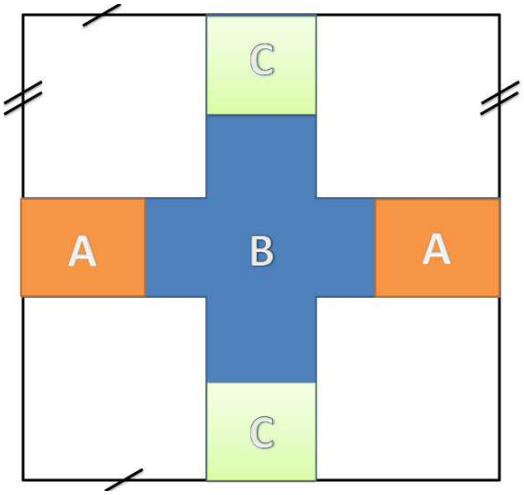

FIG. 2: A torus (the top and bottom sides and left and right sides are identified). Subregions A, B, C are defined as shown. Regions A and C are assumed to be well separated as compared to the correlation length. The regions AB and BC correspond to bipartitions of the torus into cylinders in orthogonal directions.

$$S^{\text{topo}}_{ABC} + S^{\text{topo}}_{B} - S^{\text{topo}}_{AB} - S^{\text{topo}}_{BC} \leq 0 \tag{4}$$

This inequality implies the TEEs expected from the disc is not legal for the torus.

For regions where the boundary is topologically trivial and contractible (such as ABC or B), one expects the TEE to be independent of the surface on which they are defined, and hence $S^{\text{topo}}_{ABC} = S^{\text{topo}}_{B} = -\gamma$. Only regions AB and BC, whose boundaries wrap around the torus, are sensitive to the topology of the space they are defined on. Their TEEs satisfy:

$$\gamma_{BC} + \gamma_{AB} \leq 2\gamma \tag{5}$$

where we have defined $S^{\text{topo}}_{AB(BC)} = -\gamma_{AB(BC)}$. Clearly this does not allow both the TEEs to be 2γ. In fact if one of them attains its maximal disc value, the other must vanish. Note, the TEE reduces the total entropy. Thus, when the entropy of a cut along one of the cycles of the torus attains its minimum value, i.e. we have most knowledge about the state on the cut, then along the orthogonal direction, the entropy associated with a cut must attain its maximal value, implying our knowledge is the least. Therefore this can be thought of as an uncertainty relation, between cuts that wrap around different directions of the torus.

III. EXTRACTING STATISTICS FROM TOPOLOGICAL ENTANGLEMENT ENTROPY

The modular $\mathcal{S}$ and $\mathcal{U}$ matrices describe the action of certain modular transformations on the degenerate

ground states of the topological quantum field theory. On the other hand, the braiding and statistics of quasiparticles are encoded in the $\mathcal{S}$ and $\mathcal{U}$ matrices. For Abelian phases, the ij'th entry of the $\mathcal{S}$ matrix corresponds to the phase the i'th quasi-particle acquires when it encircles the j'th quasi-particle. The $\mathcal{U}$ matrix is diagonal and the ii'th entry corresponds to the phase the i'th quasi-particle acquires when it is exchanged with an identical one. Since the MESs are the eigenstates of the nonlocal operators defined on the entanglement cut, the MESs are the canonical basis for defining $\mathcal{S}$ and $\mathcal{U}$. The modular matrices are just certain unitary transformations of the MES basis. As argued in Appendix D, the $\mathcal{S}$ matrix acts on MESs as an operator that implements $\pi/2$ rotation while the $\mathcal{U}\mathcal{S}$ matrix corresponds to $2\pi/3$ rotation of MESs.

A. Algorithm for extracting modular $\mathcal{S}$ matrix from TEE

Since the MES states carry definite quasiparticle quantum number, the modular $\mathcal{S}$ matrix may be expressed as [3]

$$\mathcal{S}_{\alpha\beta} = \frac{1}{D}\left\langle \Xi_\alpha^{\hat{x}} | \Xi_\beta^{\hat{y}} \right\rangle \tag{6}$$

Here D is the total quantum dimension and $\hat{x}$ and $\hat{y}$ are two directions on a torus. Eqn.6 is just a unitary transformation between the particle states along different directions. In the case of a system with square geometry, the $\mathcal{S}$ matrix acts as a $\pi/2$ rotation on the MES basis $\left|\Xi_\beta^{\hat{y}}\right\rangle$. In general, however, $\hat{x}$ and $\hat{y}$ do not need to be geometrically orthogonal, and the system does not need to be rotationally symmetric, as long as the loops defining $\left|\Xi_\alpha^{\hat{x}}\right\rangle$ and $\left|\Xi_\beta^{\hat{y}}\right\rangle$ interwind with each other. Therefore, the modular $\mathcal{S}$ matrix can be derived even without any presumed symmetry of the given wave functions. Note that there is an undetermined phase for each $\left|\Xi_\alpha^{\hat{x}}\right\rangle$ and $\left|\Xi_\beta^{\hat{y}}\right\rangle$, therefore a phase freedom between the rows (columns), which may be fixed by the existence of an identity particle.

Let's start with the two primitive vectors $\vec{w}_1$ and $\vec{w}_2$ that define a torus (Fig.3) and determine the transformation of the MESs of $\vec{w}_2$ to those of $\vec{w}_2'$ given by:

$$\begin{aligned} \vec{w_1'} &= n_1\vec{w}_1 + m_1\vec{w}_2 \\ \vec{w_2'} &= n_2\vec{w}_1 + m_2\vec{w}_2 \end{aligned} \tag{7}$$

With $n_1m_2 - m_1n_2 = 1$ by definition of the modular transformation. We restrict $n_2 = -1$, which means the cross product:

$$\vec{w}_2 \times \vec{w}_2' = -\vec{w}_2 \times \vec{w}_1 = \vec{w}_1 \times \vec{w}_2 = A \tag{8}$$

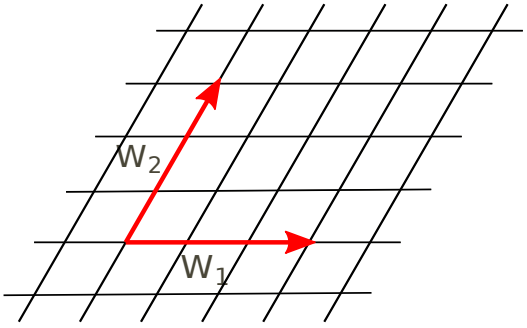

FIG. 3: Vectors $\vec{w}_1$ and $\vec{w}_2$ define a lattice with periodic boundary conditions. That is, points differing by integer linear combinations of $\vec{w}_1$ and $\vec{w}_2$ are to be identified as the same point. The area of the lattice is $|\vec{w}_1 \times \vec{w}_2|$ where $\times$ denotes the cross product.

A is the (signed) surface area of the torus.

The corresponding modular matrix can be expanded as:

$$\begin{aligned} \begin{pmatrix} n_1 & 1-n_1m_2 \\ -1 & m_2 \end{pmatrix} &= \begin{pmatrix} 1 & -n_1 \\ & 1 \end{pmatrix}\begin{pmatrix} & 1 \\ -1 & \end{pmatrix}\begin{pmatrix} 1 & -m_2 \\ & 1 \end{pmatrix} \\ &= U^{-n_1}SU^{-m_2} \end{aligned}$$

Correspondingly, according to Appendix D the transformation:

$$\mathcal{R} = \mathcal{U}^{-n_1}\mathcal{S}\mathcal{U}^{-m_2}$$

Because $\mathcal{U}$ matrix is diagonal by definition, its left (right) matrix product only adds an additional phase factor to each row (column) and can be eliminated. Therefore, without any argument on the symmetry, the generalized algorithm:

1. Given a set of ground state wave functions $|\xi_\alpha\rangle$, calculate the TEE of an entanglement bipartition along w_2 direction, for a linear combination $|\Phi\rangle = \sum c_\alpha |\xi_\alpha\rangle$. Search for the minimum of TEE $2\gamma - \gamma'$ in the c_α parameter space. That gives one MES $|\Xi_\beta\rangle$ and the corresponding quantum dimension $2\log(d_\beta) = 2\gamma - \gamma'$. Note that the existence of an identity particle ensures at least one minimum TEE $2\gamma - \gamma' = 0$.

2. iterate step 1 but with c_α in the parameter space orthogonal to all previous obtained MESs $|\Xi_\beta\rangle$. Continue this process until we have the expressions for all $|\Xi_\beta\rangle$. This gives a unitary transformation matrix U_1 with the $\alpha\beta$'th entry being $c_{\alpha\beta}$, which changes the basis from $|\xi_\alpha\rangle$ to $|\Xi_\beta\rangle$. Note that there is a relative $U(1)$ phase degree of freedom for each $|\Xi_\beta\rangle$.

3. Repeat step 1 and step 2 but with the entanglement cut along w_2' direction, which satisfies Eqn. 7 and

Eqn. 8, and obtains the unitary transformation matrix U_2.

4. The modular $\mathcal{S}$ matrix is given by $U_2^{-1}U_1$ except for an undetermined phase for each MES corresponding to a row or a column. The existence of an identity particle that obtains trivial phase encircling any quasi-particle helps to fix the relative phase between different MESs, requiring the entries of the first row and column to be real and positive. This completely defines the modular $\mathcal{S}$ matrix.

The above algorithm is able to extract the modular transformation matrix $\mathcal{S}$ and hence braiding and mutual statistics of quasi-particle excitations just using the ground-state wave functions as an input. Further, there is no loss of generality for non-Abelian phases, which can be dealt by enforcing the orthogonality condition in step 2 which guarantees that one obtains states with quantum dimensions d_α in an increasing order.

In Appendix E we take the square lattice toric code model as an example once again, but without presuming any symmetry of the system.

B. Extracting other modular matrices from TEE

In Appendix E, we calculate the $\mathcal{U}$ matrix for the Z_2 toric code model, given the simple action of $\mathcal{U}$ on $|\xi_{ab}\rangle$. Though we were unable to find a general algorithm for the $\mathcal{U}$ matrix, as we did for the the $\mathcal{S}$ matrix in the last subsection, in the presence of certain symmetries $\mathcal{U}$ can indeed be extracted given a set of ground-state wave functions $|\xi_\alpha\rangle$. This is achieved by first calculating the action $\mathcal{R}$ on the states $|\xi_\alpha\rangle$ under this symmetry operation, and then translating it into the action on MESs. Specifically, the corresponding modular matrix is given by $U^\dagger \mathcal{R} U$, where the unitary matrix U is obtained through the first two steps of the algorithm in the last subsection.

The aforementioned symmetry to extract $\mathcal{S}$ matrix is the $\pi/2$ rotation, as shown in Sec. IV A 3 and the first example in Appendix E, but it may be generalized to symmetries such as rotation of other angles and even reflection symmetry (see Appendix D). More interestingly, when the symmetry operation $\mathcal{R}$ is a $2\pi/3$ rotation, one gets the $\mathcal{U}\mathcal{S}$ matrix. Hence, if one starts with an arbitrary basis $|\xi_\alpha\rangle$ for the degenerate ground state manifold of a topological order, the problem of $\mathcal{S}$ and $\mathcal{U}$ matrices can be reduced to the transformation property of chosen basis states $|\xi_\alpha\rangle$ under $\pi/2$ and $2\pi/3$ rotations and the unitary transformation that translates $|\xi_\alpha\rangle$ basis to the MESs $|\Xi_\alpha\rangle$. To illustrate this point, we extract the $\mathcal{U}\mathcal{S}$ matrix for the Z_2 gauge theory in Appendix E by putting the Z_2 toric code on triangular lattice which has $2\pi/3$ rotation symmetry.

IV. DEMONSTRATION OF THE ALGORITHM TO EXTRACT STATISTICS FROM ENTANGLEMENT

A. Revisiting Chiral Spin-Liquid: Semionic Statistics from Entanglement Entropy

In this subsection, to illustrate the state dependence of TEE, we study the entanglement properties in a lattice model of an $SU(2)$ spin-symmetric CSL on a torus. The CSL has the same topological order as the half filled Landau level $\nu = 1/2$ Laughlin state [21, 44] of bosons (these bosons can be thought of as residing at the location of spin up moments), and has two-fold degenerate ground states on the torus. Even though topological properties of CSL are well established using field-theoretic methods [3], unlike continuum Laughlin states, CSL cannot be dealt with analytically and thus provides a non-trivial demonstration of our method. In particular, the low energy theory of CSL predicts a semion which is difficult to verify in the lattice wavefunction directly. We will show that our algorithm readily demonstrates the existence of semion as an excitation in CSL, which is the main objective of this section. We note that topological order in the lattice version of CSL can be confirmed by calculating its topological entanglement entropy (TEE) numerically using Monte Carlo and verifying that it is non-zero and agrees with the field theoretical predictions [33]. The fact that we are working with a generic lattice wave function rather than an idealized zero correlation length state or a topological field theory will introduce new conceptual issues - in particular, the connection between MESs and lattice ground states will be discussed.

In sectionIV A 1 we demonstrate the ground state dependence of CSL using a Variational Monte Carlo (VMC) algoritm. In sectionIV A 2, we review the basics of CSL so as to illustrate the physical meaning of CSL MESs. Finally, sectionIV A 3 illustrates our algorithm to extract the mutual statistics of quasiparticles in CSL using the entanglement data obtained using VMC.

1. *Ground State Dependence of TEE in a Chiral Spin Liquid*

We begin by reporting the results of a numerical experiment. We extract TEE of linear combinations of the two ground states of the CSL, and show that it indeed depends systematically on the chosen linear combination, when the entanglement cut wraps around the torus. We will then predict theoretically the dependence and find excellent agreement as shown in Fig. 5.

Wave functions of an SU(2) spin symmetric CSL are obtained in the slave particle construction. We write the spins as bilinear in fermions $\vec{S} = \frac{1}{2} f_\sigma^\dagger [\vec{\sigma}]_{\sigma\sigma'} f_{\sigma'}$ and assume a chiral d-wave state for the fermions. Operationally, the spin wavefunctions are obtained by Gutzwiller projection of a $d_{x^2-y^2} + id_{xy}$ superconductor

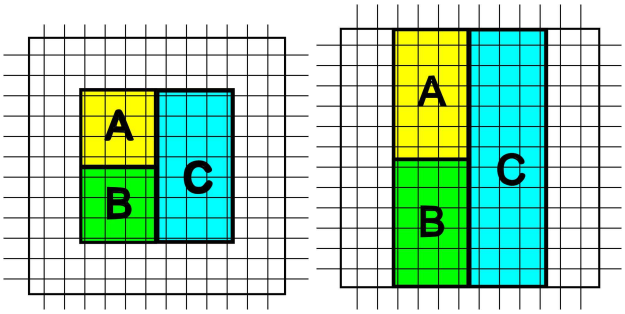

FIG. 4: The separation of the system into subsystem A, B, C and environment, periodic or antiperiodic boundary condition is employed in both $\hat{x}$ and $\hat{y}$ directions. a: The subsystem ABC is an isolated square and the measured TEE has no ground state dependence. b: The subsystem ABC takes a non-trivial cylindrical geometry and wraps around the $\hat{y}$ direction, and TEE may possess ground stated dependence.

to one fermion per site. More technical details regarding this wave function are in Appendix B. We consider the system on a torus. Before projection, one can write down different fermion states, by choosing periodic or anti-periodic boundary conditions along $\hat{x}$ and $\hat{y}$ directions. These boundary conditions are invisible to the spin degrees of freedom which are bilinear in the fermions and lead to degenerate ground states[4]. We denote the ground states by the mean field fluxes in $\hat{x}$ and $\hat{y}$ directions as $|\varphi_1, \varphi_2\rangle$, $\varphi_{1,2} = 0, \pi$. The two fold degeneracy of the CSL implies that only two of the four ground states $|0,0\rangle$, $|\pi,0\rangle$, $|0,\pi\rangle$, $|\pi,\pi\rangle$ are linearly independent. Here we consider linear combinations of $|0,\pi\rangle$ and $|\pi,0\rangle$, which we have numerically checked to be indeed orthogonal for the system sizes that we consider:

$$|\Phi(\phi)\rangle = \cos\phi\,|0,\pi\rangle + \sin\phi\,|\pi,0\rangle \tag{9}$$

We calculated TEE for the state $|\Phi\rangle$ using VMC method and Gutzwiller projected wave functions based on Eqn.B1. An efficient VMC algorithm which allows to study a linear combination of Gutzwiller projected wave functions was developed and detailed in Appendix A. To our knowledge, this is the first numerical study to accomplish this.

The geometry and partition of the system are shown in Fig. 4b. The total system size is 12 lattice spacings in both directions with rectangles A and B being 6×4 and rectangle C 12×4. Note that the subsystems AC, BC, AB, C and ABC all wrap around $\hat{y}$ direction so that their TEE will all be equal (and denoted γ'). This is the quantity we wish to access. For contractible subsystems A and B it remains the same as that expected for a region with a single boundary, cut out of a topologically trivial surface (such as a bigger disc) γ. We use the construction due to Kitaev and Preskill [15] and effectively isolate the topological contributions in the limit of small correlation length, by evaluating the combination of entropies $S_A + S_B + S_C - S_{AB} - S_{AC} - S_{BC} + S_{ABC}$. This combination is related to the TEE by:

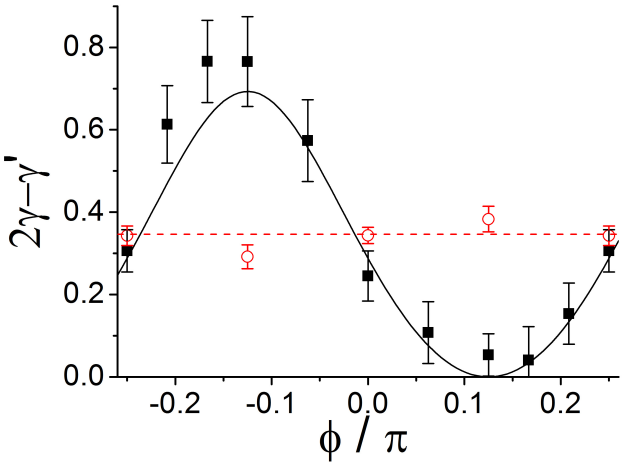

FIG. 5: The black dots show the numerically measured TEE $2\gamma - \gamma'$ for a CSL ground state from linear combination $|\Phi\rangle = \cos\phi\,|0,\pi\rangle + \sin\phi\,|\pi,0\rangle$ as a function of ϕ with VMC simulations using geometry in Fig. 4b. The solid curve is the theoretical value from Eqn. 14. The periodicity is $\pi/2$. The red dots show the TEE for the same linear combination for a trivial bipartition. In the latter case, TEE is essentially independent of ϕ and again agrees rather well with the theoretical expectation (the dashed red curve).

$$\begin{aligned} -2\gamma + \gamma' &= S_A + S_B + S_C \\ &- S_{AB} - S_{AC} - S_{BC} + S_{ABC} \\ &= 2S_A - 2S_{AC} + S_{ABC} \end{aligned} \tag{10}$$

In the second line we have exploited symmetries of the construction to reduce the problem to calculation of the Renyi entropy S_2 of three regions A, AC and ABC for each ϕ. To measure S_2 numerically, we calculated the expectation value of a $\mathrm{Swap_A}$ operator, see Ref[33] for an elaboration of the method used. Our results for $2\gamma - \gamma'(\phi)$ corresponding to different linear combinations parameterized by ϕ are shown in Fig.5. This is one of the main results of this work.

We note the TEE strongly depends on the particular linear combination chosen. The zero of the curve implies that the TEE $\gamma' = 2\gamma$, intuitive value for an entanglement cut with two boundaries. The corresponding state is the MES. We note that the MES occurs at a nontrivial angle. Understanding this requires connecting the lattice states and the field theory which is done below. We predict this angle to be 0.125π and the overall TEE dependence to be Eqn. 14, which is plotted as the solid curve Fig. 5, in rather good agreement with the numerical data.

2. Theoretical Evaluation of Ground State Dependence of TEE in CSL wavefunctions

A calculation of ground-state dependence of TEE involves two steps. In the first step, we ask the following question: given a state expressed as a linear combination of MESs, what is the expected TEE? For the CSL, this question has already been answered by Ref. 22 that TEE for a state $|\psi\rangle = a_1|1\rangle + a_2|2\rangle$ is

$$\gamma' - 2\gamma = \log\left(|a_1|^4 + |a_2|^4\right) \tag{11}$$

where $|1\rangle$, $|2\rangle$ are MESs for cutting the torus in the direction in question.

Second, we need to understand the relation between the MES and the physical states that appear in the Gutzwiller wave function. In general it appears that the only way to identify MESs in a generic wave function is by calculating the TEE. However, when the lattice model has additional symmetry, that can also be used to identify MESs. Here, we have a 12×12 system defined on a square lattice and we will exploit the $\pi/2$ rotation symmetry to establish a connection between the flux states $|\varphi_1, \varphi_2\rangle$ of the Gutzwiller ansatz and the MESs.

The Gutzwiller projected ground states of the CSL, $|0,0\rangle$ and $|\pi,\pi\rangle$ are clearly invariant under a $\pi/2$ rotation symmetry *upto a phase factor*. A simple calculation shows that the $|0,0\rangle$ state acquires phase factor -1 while the $|\pi,\pi\rangle$ state acquires no phase under rotation. Similarly, the states $\frac{1}{\sqrt{2}}\left(|0,\pi\rangle \pm |\pi,0\rangle\right)$ acquire a phase ± 1 under rotation. Having established the transformation of lattice states under rotation, we now study how the MESs in the field theory respond to rotations. We will see that $\pi/2$ rotation in the basis of the MESs is described by the modular $\mathcal{S}$ matrix. The eigenvectors of the modular $\mathcal{S}$ matrix will then be identified with lattice states that are rotation eigenstates.

The CSL has the same topological order as the half filled Landau level $\nu = 1/2$ Laughlin state [21, 44] of bosons. The field theory describing the topological order of a $\nu = 1/k$ Laughlin state is described by the following Chern-Simons action. Note, here only the very long wavelength degrees of freedom are retained:

$$S = \int \frac{k}{4\pi} a_\mu \partial_\upsilon a_\lambda \epsilon^{\mu\upsilon\lambda}$$

One can define the Wilson loop operators $T_1 = e^{i\theta_1} = e^{i\oint a_x dx}$ and $T_2 = e^{i\theta_2} = e^{i\oint a_y dy}$ around the two distinct cycles of the torus. In terms of θ_i, the action is given by

$$S = i\frac{k}{2\pi}\int dt \theta_1 \dot{\theta}_2$$

which implies that at the operator level $[\theta_1, \theta_2] = i\frac{2\pi}{k}$ or

$$T_1 T_2 = T_2 T_1 e^{2\pi i/k}$$

Owing to the above relation, there are k orthogonal ground states $|\psi_m\rangle$ that can be chosen to transform under T_i as

$$\begin{aligned} T_2|\psi_m\rangle &= e^{2\pi i(m-1)/k}|\psi_m\rangle \\ T_1|\psi_m\rangle &= |\psi_{m+1}\rangle \end{aligned}$$

In the case of a CSL phase, $k = 2$. Let us label the two degenerate ground states as $(1,0)^T$ and $(0,1)^T$, which are eigenstates of T_2:

$$\begin{aligned} T_2\,(1,0)^T &= (1,0)^T \\ T_2\,(0,1)^T &= -(0,1)^T \\ T_1\,(1,0)^T &= (0,1)^T \\ T_1\,(0,1)^T &= (1,0)^T \end{aligned}$$

The last two equations are due to the commutation relation $T_1 T_2 = -T_2 T_1$. It follows that the eigenstates of T_1 are $(1,1)^T/\sqrt{2}$ and $(1,-1)^T/\sqrt{2}$.

The significance of the $T_{1,2}$ eigenstates is that they are MESs[22], for cuts whose boundaries are parallel to the loops used to define $T_{1,2}$. This is because eigenstates of these loop operators have a fixed value of flux enclosed within the relevant cycle of the torus, which minimizes the entanglement entropy for a parallel cut.

Now consider a $\pi/2$ rotation, under which $\theta_1 \to \theta_2$ and $\theta_2 \to -\theta_1$ so $T_1 \to T_2$ and $T_2 \to T_1^{-1} = T_1$. Thus, the matrix representing the effect of $\pi/2$ rotation for CSL in T_2 eigenstate basis is:

$$\mathcal{S} = \begin{pmatrix} \frac{1}{\sqrt{2}} & \frac{1}{\sqrt{2}} \\ \frac{1}{\sqrt{2}} & -\frac{1}{\sqrt{2}} \end{pmatrix} \tag{12}$$

Note that we have used the symbol $\mathcal{S}$ for the above matrix because it is indeed the modular $\mathcal{S}$ matrix of the Chern-Simons topological quantum field theory corresponding to a CSL. We recall that the modular $\mathcal{S}$ matrix transforms the eigenstates of one Wilson loop operator T_2 to those of T_1. We will return to the discussion of deriving $\mathcal{S}$ matrix for CSL state using the entanglement properties of the ground states in Sec. IV A 3. Here we restrict ourselves to the calculation of TEE for the CSL.

Since we are interested in the entanglement entropy with respect to a cut with non-contractible boundaries, such as the one shown in Fig.1b, let us represent all our states in the basis of the eigenstates of T_2, i.e. the states $(0,1)$ and $(1,0)$. Then, by matching eigenstates of the $\mathcal{S}$ matrix in the above basis and rotation eigenstates of the lattice problem, we conclude:

$$|\pi,0\rangle = \left(\sin\frac{\pi}{8},\cos\frac{\pi}{8}\right)^T$$
$$|0,\pi\rangle = \left(\cos\frac{\pi}{8},-\sin\frac{\pi}{8}\right)^T$$

We can now expand the general linear combination state $|\Phi(\phi)\rangle$ in MESs:

$$\begin{aligned}|\Phi\rangle &= \cos\phi\,|0,\pi\rangle + \sin\phi\,|\pi,0\rangle \\ &= \left(\cos\left(\phi-\frac{\pi}{8}\right),\sin\left(\phi-\frac{\pi}{8}\right)\right) \end{aligned} \quad (13)$$

Then, according to Eqn. (2), theoretically one expects the following expression for TEE:

$$2\gamma-\gamma' = \log\frac{4}{3+\sin(4\phi)} \quad (14)$$

which is compared with the numerical data in Fig. 5. The MES occur at the value of $\phi=\pi/8 \pmod{\pi/2}$.

3. *Modular S-matrix of CSL from TEE*

Let's consider the CSL wave functions studied in Sec. IV A 1, and assume that we did not have any information about the individual quantum dimensions or the modular $\mathcal{S}$ matrix. The only information that is provided is the two-fold degenerate ground-state wave functions $|\pi,0\rangle$ and $|0,\pi\rangle$. We construct the linear combination $|\Phi\rangle$ as Eqn.13 and calculate its TEE for a non-trivial bipartition as Fig.1b on a $\pi/2$ rotation symmetric lattice. Consequently, we get the $2\gamma-\gamma'$ dependence on parameter ϕ in Fig.5.

We notice that the minimum of the $2\gamma'-\gamma$ attained is approximately zero. According to Eqn.2, this implies that at least one of the quantum dimensions d_i should be 1. Since the total quantum dimension $D=\sqrt{d_0^2+d_{1/2}^2}=\sqrt{2}$, this implies that $d_0=d_{1/2}=1$. Also, we see that the MES lies at $\phi\approx 0.14\pi$ by fitting Fig.5 to Eqn.2.

For system with square geometry the $\mathcal{S}$ matrix describes the action of $\pi/2$ rotation on the MESs. Since the two states $|0,\pi\rangle$ and $|\pi,0\rangle$ transform into each other under $\pi/2$ rotation, this implies that in the basis $\{|0,\pi\rangle,|\pi,0\rangle\}$, the modular $\mathcal{S}$ matrix is given by the Pauli matrix σ_x. To change the basis to MESs, we just need a unitary transformation V that rotates $|0,\pi\rangle\,|\pi,0\rangle$ basis to the MESs basis. The V is determined by the fact that one needs to rotate $|0,\pi\rangle\,|\pi,0\rangle$ basis by an angle $\approx 0.14\pi$ to obtain MES (this is the numerically determined value, the exact value being $\pi/8$). Therefore,

$$\mathcal{S}=V^\dagger\begin{pmatrix}0&1\\1&0\end{pmatrix}V$$

where

$$V\approx\begin{pmatrix}\cos(0.14\pi) & -\sin(0.14\pi)e^{i\varphi}\\ \sin(0.14\pi) & \cos(0.14\pi)e^{i\varphi}\end{pmatrix}$$

from the two MESs: $(\cos(0.14\pi),\sin(0.14\pi))^T$ and $(-\sin(0.14\pi),\cos(0.14\pi))^T$ and φ is an undecided phase. This yields the following value for the approximate modular $\mathcal{S}$ matrix

$$\mathcal{S}\approx\begin{pmatrix}\sin(0.28\pi) & \cos(0.28\pi)e^{i\varphi}\\ \cos(0.28\pi)e^{-i\varphi} & -\sin(0.28\pi)\end{pmatrix}$$

The existence of an identity particle requires positive real entries in the first row and column and implies $\varphi=0$, which gives:

$$\mathcal{S}\approx\begin{pmatrix}0.77 & 0.63\\ 0.63 & -0.77\end{pmatrix}$$

Comparing this result with the exact expression in Eqn. 12, we observe that even though the $\mathcal{S}$ matrix obtained using our method is approximate, some of the more important statistics can be extracted exactly. In particular, the above $\mathcal{S}$ matrix tells us that the quasi-particle corresponding to $d_0=1$ does not acquire any phase when it goes around any other particle and corresponds to an identity particle as expected, while the quasi-particle corresponding to $d_{1/2}=1$ has semion statistics since it acquires a phase of π when it encircles another identical particle. Numerical improvements can further reduce the error in pinpointing the MES and thereby leading to a more accurate value of the $\mathcal{S}$ matrix. As another application, we study the action of modular transformation on the MESs $|\Xi_\alpha\rangle$ for the Z_2 gauge theory in Appendix E.

B. Toric code model: A Pedagogical Illustration of the Algorithm

In this subsection we use the Kitaev's Toric code model [11] as a pedagogical example to understand ground-state dependence of TEE and the nature of the MESs for a Z_2 gauge theory.

Consider the toric code Hamiltonian of spins defined on the links of a square lattice[11]:

$$H=-\sum_s A_s-\sum_p B_p \quad (15)$$

where s and p represent the links spanned by star and plaquette as shown in the Fig.6, and $A_s=\prod_{j\in s}\sigma_j^x$, $B_p=\prod_{j\in p}\sigma_j^z$. Since all individual terms in the Hamiltonian commute with each other, ground states are constructed from the simultaneous eigenstates of all A_s and

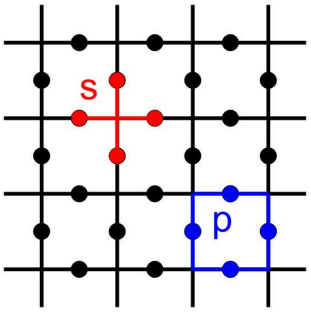

FIG. 6: Illustration of a lattice of the toric code model, the links spanned by star and plaquette are highlighted in red and blue, respectively.

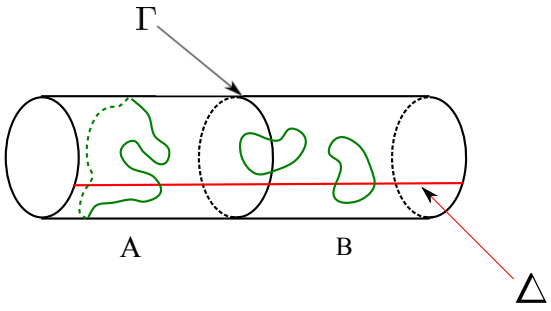

FIG. 7: A snapshot of the ground state on the cylinder. Closed-loop strings ("Z_2 electric fields") can wrap around the cylinder. The ground states are doubly degenerate, corresponding to even and odd winding number sectors. The total number of string crossings the cut Δ equals the winding number, modulo 2. The number of strings crossing at the boundary Γ is even in the degenerate ground states.

B_p. Define the operator $W^z(C)$ associated with a set of closed curves C on the bonds of the lattice, as follows

$$W^z(C) \;=\; \prod_{j\in C}\sigma_j^z \tag{16}$$

Then the ground state is an equal superposition of all possible loop configurations: $\sum_C W^z_{ab}(C)|\mathrm{vac}_x\rangle$, where $|\mathrm{vac}_x\rangle$ is a state with $\sigma_x=-1$ on every site. The closed loops are interpreted as electric field lines of the Z_2 gauge theory. We now consider two geometries, first the cylinder and then the torus. The former case has a pair of degenerate ground states, and is the simplest setting to demonstrate state dependence of TEE.

1. *Cylinder Geometry*

On a cylinder, the Hamiltonian in Eqn.15 leads to a pair of degenerate ground states (the A_s part of the Hamiltonian is suitably modified at the boundary of the cylinder to only include three links). The two normalized ground states $|\xi_0\rangle, |\xi_1\rangle$, are given by equal superpositions of electric field loop configurations which have an even and odd winding number around the cylinder respectively (see Fig. 7). Consider now partitioning the cylinder into two cylindrical regions A and B. Then the Schmidt decomposition of these ground states can be written as:

$$\begin{aligned}
|\xi_0\rangle &= \frac{1}{\sqrt{2N_q}}\sum_{\{q_l\}}\left(|\Psi^A_{\{q_l\},0}\rangle|\Psi^B_{\{q_l\},0}\rangle + |\Psi^A_{\{q_l\},1}\rangle|\Psi^B_{\{q_l\},1}\rangle\right)\\
|\xi_1\rangle &= \frac{1}{\sqrt{2N_q}}\sum_{\{q_l\}}\left(|\Psi^A_{\{q_l\},0}\rangle|\Psi^B_{\{q_l\},1}\rangle + |\Psi^A_{\{q_l\},1}\rangle|\Psi^B_{\{q_l\},0}\rangle\right)
\end{aligned} \tag{17}$$

where the N_q distinct configurations represented by $\{q_l\}$ denote the electric field configurations at the cut. The number of field lines crossing the cut is always even, since the ground state is composed of closed loops. For trivial bipartitions, this exhausts all terms in the Schmidt decomposition [14]. However, given that the boundary of the cut is non-contractible, the additional index 0, 1 appears which counts the parity of electric field winding around the cylinder, within a partition. These are correlated between the two partitions, for the fixed winding number ground states. This is the key difference from a trivial bipartition, leading to the ground-state dependence of TEE.

We now calculate the entanglement entropy associated with such a cut for an arbitrary linear combination of these two ground states $|\Psi\rangle = c_0|\xi_0\rangle + c_1|\xi_1\rangle$, with unit norm. Using Eqn. 17 one can easily verify:

$$\begin{aligned}
|\Psi\rangle = \frac{1}{\sqrt{2N_q}}\sum_{\{q_l\}} \quad & [(c_0+c_1)|\Psi^A_{\{q_l\},+}\rangle|\Psi^B_{\{q_l\},+}\rangle\\
+ \quad & (c_0-c_1)|\Psi^A_{\{q_l\},-}\rangle|\Psi^B_{\{q_l\},-}\rangle]
\end{aligned} \tag{18}$$

where $|\Psi^{A(B)}_{\{q_l\},\pm}\rangle = \left(|\Psi^{A(B)}_{\{q_l\},0}\rangle \pm |\Psi^{A(B)}_{\{q_l\},1}\rangle\right)/\sqrt{2}$. For a Schmidt decomposition $|\Psi\rangle = \sum_a \sqrt{\lambda_a}|\Psi^A_a\rangle|\Psi^B_a\rangle$ the nth Renyi entropy is given by: $S_n = \frac{1}{1-n}\log\left(\sum_a \lambda_a^n\right)$. We arrive at: $S_n = \frac{1}{1-n}\log N_q^{1-n}[p_+^n + p_-^n]$, where $p_\pm = |c_0 \pm c_1|^2/2$. Recognizing that the closed loop constraint leads to $N_q = 2^{L-1}$, where L is the length of the cut, and using the definition of TEE in Eqn. 1 we have:

$$\gamma_n' = \log 2 - \frac{1}{1-n}\log(p_+^n + p_-^n) \tag{19}$$

Thus, for the electric field winding eigenstates $|\xi_{0,1}\rangle$ where $p_\pm = 1/2$, the TEE vanishes. However, for their equal superpositions when one of p_+ or p_- vanishes, the TEE attains its maximal value $\log 2$. These are eigenstates of the Wilson loop operator that encircles the cylinder and measures the Z_2 magnetic flux (vison number) threading it. An example of such a flux operator is $F = \prod_{j\in Q}\sigma_j^z$, where Q is a closed curve that loops once

around the cylinder, such as the boundary Γ in Fig. 7. Since TEE reduces the entanglement entropy, the maximum TEE states correspond to MESs. Why these MESs are eigenstates of flux through the cylinder for this particular cut? The number of electric field lines crossing the boundary Γ is always even. This constraint carries some information and hence lowers the entropy by bringing in the standard TEE of $\log 2$. On the other hand, the topology of the cut boundary Γ allows for a determination of which magnetic flux sector the cylinder is in. A state that is not an eigenstate of magnetic flux through the cylinder leads to a loss of information and hence a positive contribution to the total entanglement entropy (and reduces TEE). This suggests that the MESs are eigenstates of loop operators which can be defined parallel to the cut Γ. This is further substantiated by the result for the torus case discussed below, where they are simultaneous eigenstates of magnetic flux enclosed by the cut and electric flux penetrating the cut.

2. Torus Geometry

The four degenerate ground states are distinguished by the even-odd parity of the winding number of electric field lines around the two cycles of the torus. The operator $W^z(C)$, which generates the set of closed loops C can be used to write the ground states:

$$|\xi_{ab}\rangle = \sum_C W^z_{ab}(C)|\mathrm{vac}_x\rangle$$

where the subscript a (b) takes on binary values $0, 1$ and denotes whether the loops C belong to the even or odd winding number sectors along the $\hat{x}$ ($\hat{y}$) direction, and $|\mathrm{vac}_x\rangle$ is a state with $\sigma_x = -1$ on every site. The four ground states cannot be mixed by any local operator and hence realize a Z_2 topological order. Let us consider a ground state as the following linear combination:

$$|\Psi\rangle = \sum_{a,b=0,1} c_{a,b}\,|\xi_{ab}\rangle \tag{20}$$

We are interested in calculating entanglement entropy for the state $|\Psi\rangle$ corresponding to the partition shown in the Fig.1b and the dependence of TEE on parameters $c_{a,b}$. After straightforward algebra (see details in Appendix C), one finds the following expression for subsystem A with boundaries of length L:

$$S_n = L\log(2) - \gamma'_n$$

where

$$\gamma'_n = 2\log\,(2) - \frac{1}{1-n}\log\sum_{j=1}^{4} p_j^n \tag{21}$$

and

$$\begin{aligned} p_1 &= \frac{|c_{00}+c_{01}|^2}{2} \\ p_2 &= \frac{|c_{00}-c_{01}|^2}{2} \\ p_3 &= \frac{|c_{10}+c_{11}|^2}{2} \\ p_4 &= \frac{|c_{10}-c_{11}|^2}{2} \end{aligned} \tag{22}$$

This is indeed consistent with Eqn.2, given that $\gamma = \log D = \log 2$ and $d_j = 1$ for an Abelian topological order with $D^2 = 4$ degenerate ground states. Further, Eqn.21 readily leads to the following four MESs:

$$\begin{aligned} |\Xi_1\rangle &= \frac{1}{\sqrt{2}}(|\xi_{00}\rangle + |\xi_{01}\rangle) \\ |\Xi_2\rangle &= \frac{1}{\sqrt{2}}(|\xi_{00}\rangle - |\xi_{01}\rangle) \\ |\Xi_3\rangle &= \frac{1}{\sqrt{2}}(|\xi_{10}\rangle + |\xi_{11}\rangle) \\ |\Xi_4\rangle &= \frac{1}{\sqrt{2}}(|\xi_{10}\rangle - |\xi_{11}\rangle) \end{aligned} \tag{23}$$

What is the physical significance of these four states being the MESs? Similar to the cylinder geometry case, these states are the simultaneous eigenstates of Wilson loop operator that encircles the torus and measures the Z_2 magnetic and electric fluxes threading it, as shown in Table I and Fig.8. We leave more detailed algebra to Appendix C.

When γ'_n is maximized, the corresponding S_n is minimized, providing the maximum possible information about a given state. Since the cut is made along $\hat{y}$, it can measure the Z_2 magnetic and electric fluxes directed parallel to $\hat{x}$. Hence the MES $|\Xi_\alpha\rangle$ with definite magnetic and electric flux sectors, maximizes the TEE with $\gamma_{topo} = 2\log(2)$, a contribution of $\log(2)$ from each of the two boundaries. Linear superposition of different MESs $|\Xi_\alpha\rangle$, scrambles the information obtained from magnetic and electric sectors; especially, at the extreme case of equal superposition of $|\Xi_\alpha\rangle$, all information about the global quantum numbers has been lost and we have $\gamma' = 0$. This offers another example where MESs are the eigenstates of loop operators defined on the cylinder from the entanglement cut.

V. CONCLUSION

In this paper, we demonstrated that on general grounds, the entanglement entropy of topologically ordered phases depends on the ground state when the entanglement cut is non-contractible. Furthermore, we showed that this dependence can be used to extract

MES	T_y	F_y	quasi-particle
Ξ_1	0	0	1
Ξ_2	1	0	m
Ξ_3	0	1	e
Ξ_4	1	1	em

TABLE I: List of Z_2 magnetic flux T_y, Z_2 electric flux F_y and corresponding quasi-particle of Wilson loop operator for the four MESs $|\Xi_\alpha\rangle$ of the toric code with system geometry in Fig.1b. The definitions of T_y and F_y are in Appendix C.

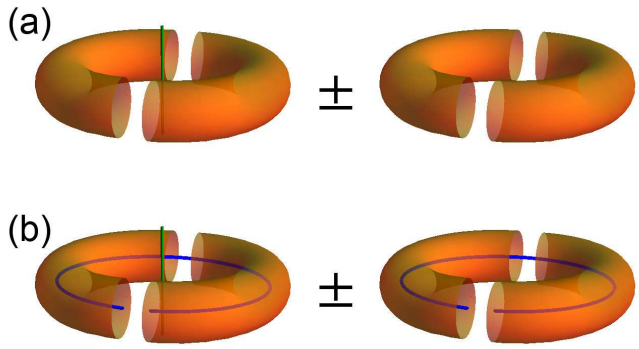

FIG. 8: The four minimum entropy states of the Z_2 topological phase corresponding to the bipartition shown in the figure expressed as linear combinations of the four magnetic flux states. The magnetic π flux is represented by the thick blue and green lines.

braiding and statistics of the anyonic quasiparticles in the topological phase. We also developed an efficient Variational Monte Carlo (VMC) algorithm to implement our algoritm to extract braiding and statistics of quasiparticles. We illustrated the general algorithm by studying two well-known topologically ordered phases, the chiral spin liquid (CSL) and the Z_2 spin liquid using VMC method and the Z_2 toric code model analytically. We also introduced the concept of minimum entropy states (MESs) and explained their physical significance.

We note that our algorithm is completely different than the use of entanglement spectra [38] to extract universal properties of a topological phase. In particular, our algorithm is valid for all topologically ordered states, including those that do not have any edge states, such as Toric code model. In this context, we note that if edge states do exist, then the modular matrices extracted using our algorithm also determine the central charge of the edge state modulo 8 [18]. Given the ground states, this algorithm determines the topological order to a large extent. We note that Wen proposed a different way to extract $\mathcal{S}$ and $\mathcal{U}$ matrices by calculating the non-abelian Berry phase [3] which in practice may be difficult to implement, especially on a lattice, since it requires calculating the degenerate ground states ψ_n of the system as function of the modular parameter $\tau = \omega_2/\omega_1$ and calculating the derivatives such as $\langle\psi_n(\tau)|\partial_\tau|\psi_m(\tau)\rangle$.

We note that there may be cases where the $\pi/2$ and $2\pi/3$ rotations of the MESs may not be exactly identifiable with the modular $\mathcal{S}$ and $\mathcal{US}$ matrices respectively. This may happen, for example, when the particles have an internal angular momentum which may cause the wavefunction to acquire an additional phase upon rotation, over and above the phase due to underlying topological structure. If the MESs correspond to spin-singlet spin-liquid wave functions (such as CSL studied in this paper) and/or string-net models (such as toric code model) where there is no such internal structure, there should not be such additional phase. Further, since all MESs are locally same, they should all acquire same extra phase due to any local physics and therefore, the extra phase may be separable from the topological phase.

For quantum Hall systems, because of the bulk-edge correspondence, the fusion algebra and topological spin of the bulk quasi-particles also determine the fusion rules and scaling dimensions for the primary fields in the chiral CFT at the edge. Therefore, in the context of quantum Hall systems, the entanglement entropy of the ground state manifold determines robust features of the fields in the corresponding edge CFT.

It would also be interesting to consider generalization of the methods developed in our paper to higher dimensions. Discrete gauge theories furnish the best known theories with long-range entanglement in $D \geq 3$ dimensions and akin to $D = 2$, they again support degenerate ground states on the torus. It is known that these these theories again have non-zero TEE that is proportional to $\log(|G|)$, the number of elements in the gauge group [45, 46]. A simple generalization of the method developed in this paper shows that TEE for bipartition that has non-contractible boundaries will again depend on the ground state, and one will again find certain MESs that have the maximum knowledge of the quantum numbers associated with an entanglement cut. Yet we are not aware of simple generalization of modular transformations to higher dimensions, the meaning of the matrix that relates MESs for orthogonal entanglement cuts in higher dimensions requires further investigation.

Acknowledgements: We thank Alexei Kitaev, Michael Levin, Chetan Nayak and Shinsei Ryu for helpful discussions. A part of this research was performed at Kavli Institute for Theoretical Physics, University of California Santa Barbara, supported by the National Science Foundation under Grant No. NSF PHY05-51164. M. O. was supported in part by Grant-in-Aid for Scientific Research (KAKENHI) No. 20102008. Y. Z., T.G. and A. V. were supported by NSF DMR-0645691.

Appendix A: Variational Monte Carlo method for a linear combination of wave-functions

To calculate TEE for wave functions of different linear combinations, it is important to establish a VMC algo-

rithm for wave function as $|\Phi\rangle = \cos\phi\,|\Phi_1\rangle + \sin\phi\,|\Phi_2\rangle$, where we assume $|\Phi_1\rangle$ and $|\Phi_2\rangle$ are properly normalized. In our case, $|\Phi_1\rangle$ and $|\Phi_2\rangle$ are two degenerate ground states, $\langle\alpha|\Phi_1\rangle$ and $\langle\alpha|\Phi_2\rangle$ are single Slater determinants products for each configuration $|\alpha\rangle$, making $\langle\alpha|\Phi\rangle$ a sum of two Slater determinants products. However, it may also be generalized to the situation of any wave functions.

In the VMC scenario, the central quantity to evaluate in each Monte Carlo step is the ratio of $\langle\alpha'|\Phi\rangle\,/\,\langle\alpha|\Phi\rangle$, which now has the form:

$$\frac{\langle\alpha'|\Phi\rangle}{\langle\alpha|\Phi\rangle} = \frac{\cos\phi\,\langle\alpha'|\Phi_1\rangle + \sin\phi\,\langle\alpha'|\Phi_2\rangle}{\cos\phi\,\langle\alpha|\Phi_1\rangle + \sin\phi\,\langle\alpha|\Phi_2\rangle} \tag{A1}$$

It is usually much less costly to calculate ratio of $\langle\alpha'|\Phi_1\rangle\,/\,\langle\alpha|\Phi_1\rangle$ and $\langle\alpha'|\Phi_2\rangle\,/\,\langle\alpha|\Phi_2\rangle$ if $|\alpha\rangle$ and $|\alpha'\rangle$ are locally different. For our case, when $|\alpha\rangle$ and $|\alpha'\rangle$ differ only by one spin(electron) exchange, a much less costly and more accurate algorithm may be implemented for the ratio of determinants with only one different row or column. Unfortunately, after linear superposing different $|\Phi_i\rangle$, Eqn.A1 no longer has such a privilege.

However, one can re express Eqn.A1 as:

$$\frac{\langle\alpha'|\Phi\rangle}{\langle\alpha|\Phi\rangle} = \frac{a + bc\cdot\tan\phi}{1 + c\cdot\tan\phi}$$

where

$$\begin{aligned} a &= \langle\alpha'|\Phi_1\rangle\,/\,\langle\alpha|\Phi_1\rangle \\ b &= \langle\alpha'|\Phi_2\rangle\,/\,\langle\alpha|\Phi_2\rangle \end{aligned}$$

are again ratio of determinants and can be effectively evaluated, and

$$c = \langle\alpha|\Phi_2\rangle\,/\,\langle\alpha|\Phi_1\rangle$$

can be efficiently kept track of with $c' = a^{-1}bc$ whenever the update $|\alpha\rangle \to |\alpha'\rangle$ is accepted in a Monte Carlo step. In practice, numerical check should be included to make sure error for c does not accumulate too much after a certain number of Monte Carlo steps.

This algorithm may be easily generalized to the linear combination of n wave functions, with the computational cost only n times that for a single wave functions.

Appendix B: Variational wave function for Chiral Spin Liquid

Chiral Spin Liquid From Gutzwiller Projection: The lattice wave function for the CSL states that we consider are obtained using the slave-particle formalism by Gutzwiller projecting a $d+id$ BCS state [21, 44]. Specifically, we Gutzwiller project the ground state of the following Hamiltonian of electrons hopping on a square lattice at half filling:

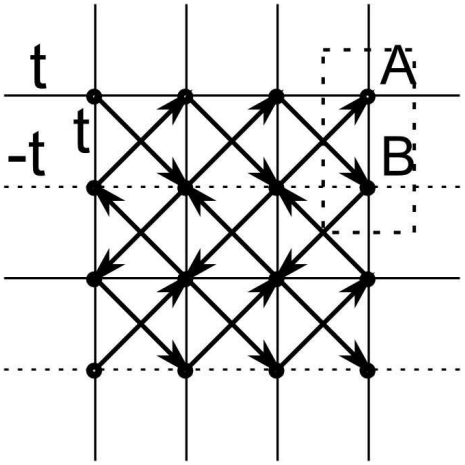

FIG. 9: Illustration of a square lattice hopping model connected with a $d+id$ superconductor. While the nearest neighbor hopping is along the square edges with amplitude t ($(-t)$ for hopping along dash lines), the second nearest neighbor hopping is along the square diagonal (arrows in bold), with amplitude $+i\Delta$ ($-i\Delta$) when hopping direction is along (against) the arrow. The two sublattices in the unit cell are marked as A and B.

$$H = \sum_{\langle ij\rangle} t_{ij} c_i^\dagger c_j + i\sum_{\langle\langle ik\rangle\rangle} \Delta_{ik} c_i^\dagger c_k \tag{B1}$$

Here i and j are nearest neighbors and the hopping amplitude t_{ij} is t along the $\hat{y}$ direction and alternating between t and $-t$ in the $\hat{x}$ direction from row to row; and i and k are second nearest neighbors connected by hoppings along the square lattice diagonals, with amplitude $i\Delta_{ik} = i\Delta$ along the arrows and $i\Delta_{ik} = -i\Delta$ against the arrows, see Fig.9. The unit cell contains two sublattices A and B. This model leads to a gapped state at half filling and the resulting valence band has unit Chern number. This hopping model is equivalent to a $d+id$ BCS state by an $SU(2)$ Gauge transformation. We take $\Delta = 0.5t$ to maximize the relative size of the gap and minimize the finite size effect. Please refer to Ref[33] for further details regarding the exact form of the wave function.

Appendix C: Minimum entropy states of Toric code model on dividing torus

In this appendix we Schmidt-decompose the individual Toric code ground states $|\Psi\rangle$ in Eqn.20 for the bipartition of a torus in Fig.1b. It is helpful to introduce a virtual cut Δ which wraps around the torus in the $\hat{x}$ direction, and define $\left|\Psi^{A(B)}_{\{q_l\},b}\right\rangle$ as the normalized equal superposition

of all the possible configurations of closed-loop strings C in the subsystem A (B) with the partition boundary condition specified by $\{q_l = 0, 1\}$, $l = 1, 2, ..., L$(so L is the total length of the boundary), and the number of crossings of the virtual cut Δ modulo 2 equals $b = 0, 1$. The four ground states may now be expanded as

$$|\xi_{ab}\rangle = \frac{1}{\sqrt{2N_q}} \sum_{\{q_l\}\in a} \Big(|\Psi^A_{\{q_l\},0}\rangle |\Psi^B_{\{q_l\},b}\rangle + |\Psi^A_{\{q_l\},1}\rangle |\Psi^B_{\{q_l\},(b+1) \bmod 2}\rangle \Big)$$

Here $\{q_l\} \in a = 0$ (1) denotes that the only even (odd) number of crossings are allowed at the boundary Γ_1 (the number of crossings at the other boundary Γ_2 must be same modulo 2). $N_q = 2^{L-2}$ equals the total number of valid boundary conditions $\{q_l\} \in a$ in each parity sector.

We calculate entanglement entropy using the reduced density matrix. Here, $\rho^A = \mathrm{tr}_B |\Psi\rangle\langle\Psi|$ is readily calculated,

$$\begin{aligned}
\rho^A &= \frac{1}{2N_q} \sum_{\{q_l\}\in \text{even}} \Big[\left(|c_{00}|^2 + |c_{01}|^2\right) \Big(|\Psi^A_{\{q_l\},0}\rangle\langle\Psi^A_{\{q_l\},0}| \\
&\quad + |\Psi^A_{\{q_l\},1}\rangle\langle\Psi^A_{\{q_l\},1}| \Big) \\
&\quad + 2\,\mathrm{Real}(c^*_{00}c_{01}) \Big(|\Psi^A_{\{q_l\},0}\rangle\langle\Psi^A_{\{q_l\},1}| + |\Psi^A_{\{q_l\},1}\rangle\langle\Psi^A_{\{q_l\},0}| \Big) \Big] \\
&\quad + \frac{1}{2N_q} \sum_{\{q_l\}\in \text{odd}} \Big[\left(|c_{10}|^2 + |c_{11}|^2\right) \Big(|\Psi^A_{\{q_l\},0}\rangle\langle\Psi^A_{\{q_l\},0}| \\
&\quad + |\Psi^A_{\{q_l\},1}\rangle\langle\Psi^A_{\{q_l\},1}| \Big) \\
&\quad + 2\,\mathrm{Real}(c^*_{10}c_{11}) \Big(|\Psi^A_{\{q_l\},0}\rangle\langle\Psi^A_{\{q_l\},1}| + |\Psi^A_{\{q_l\},1}\rangle\langle\Psi^A_{\{q_l\},0}| \Big) \Big] \\
&= \frac{1}{2N_q} \sum_{\{q_l\}\in \text{even}} \Big[|c_{00} + c_{01}|^2 |\Psi^A_{\{q_l\},+}\rangle\langle\Psi^A_{\{q_l\},+}| \\
&\quad + |c_{00} - c_{01}|^2 |\Psi^A_{\{q_l\},-}\rangle\langle\Psi^A_{\{q_l\},-}| \Big] \\
&\quad + \frac{1}{2N_q} \sum_{\{q_l\}\in \text{odd}} \Big[|c_{10} + c_{11}|^2 |\Psi^A_{\{q_l\},+}\rangle\langle\Psi^A_{\{q_l\},+}| \\
&\quad + |c_{10} - c_{11}|^2 |\Psi^A_{\{q_l\},-}\rangle\langle\Psi^A_{\{q_l\},-}| \Big]
\end{aligned}$$

Here $|\Psi^A_{\{q_l\},\pm}\rangle = \frac{1}{\sqrt{2}} \Big(|\Psi^A_{\{q_l\},0}\rangle \pm \Psi^A_{\{q_l\},1}\rangle \Big)$ and hold the orthogonal condition.

From the above expression, it immediately follows that the Renyi entanglement entropy S_n is given by Eqn.21:

$$\begin{aligned}
S_n &= \frac{1}{1-n} \log\left(Tr\rho^n_A\right) \\
&= \frac{1}{1-n} \log\left(\left(\frac{1}{2N_q}\right)^n \cdot N_q \left(\sum_{j=1}^4 (2p_j)^n \right) \right) \\
&= \log N_q + \frac{1}{1-n} \log \sum_{j=1}^4 p_j^n \\
&= L\log 2 - \left(2\log 2 + \frac{1}{n-1} \log \sum_{j=1}^4 p_j^n \right)
\end{aligned}$$

where p_j are defined in Eqn. 22.

To understand the nature of the corresponding MES in Eqn. 23, we first discuss the quasi-particle excitations of the Toric code model. Imagine acting a string operator defined on the links of the lattice

$$W^z(O) = \prod_{j\in O} \sigma^z_j$$

Now $W^z(O)|\mathrm{vac}_x\rangle$ is an excited states and still an eigenstate of A_s and B_p, with $A_s = -1$ at the two ends of O. We may regard them as electric charge quasi-particles that cost a finite energy to create and the string connecting them as an electric field line. To return to the ground state, the electric charges need to be annihilated with each other. One way to do this is to wrap the open string O parallel to $\hat{x}$ around the cycle of the torus. O becomes a closed loop C, yet this changes the parity of electric field winding number along $\hat{x}$. We define the electric charge loop operator that insert an additional electric field in the $\hat{x}(\hat{y})$ direction by the above procedure as a Z_2 electric flux insertion operator $T_x(T_y)$.

$$\begin{aligned}
T_x|\xi_{1b}\rangle &= |\xi_{0b}\rangle \\
T_x|\xi_{0b}\rangle &= |\xi_{1b}\rangle \\
T_y|\xi_{a1}\rangle &= |\xi_{a0}\rangle \\
T_y|\xi_{a0}\rangle &= |\xi_{a1}\rangle
\end{aligned} \tag{C1}$$

There is also a magnetic field, which determines the phase of the electric charge as it moves. In particular, when there is a magnetic field along the $\hat{y}$ direction of the torus of 1(0) total flux($mod 2$), the electric charge picks up a $-(+)$ sign traveling around the loop around the $\hat{x}$ direction, and similarly for the magnetic field along the $\hat{x}$ direction. Denoting the insertion operator of such Z_2 magnetic flux as F_y and F_x, the loop operators of the magnetic charge (vison), we have,

$$\begin{aligned}
T_x F_y &= -F_y T_x \\
T_y F_x &= -F_x T_y
\end{aligned}$$

They suggest that $T_x(T_y)$ is the magnetic flux measuring operator in the $\hat{y}(\hat{x})$ direction and $F_x(F_y)$ is the electric flux measuring operator in the $\hat{y}(\hat{x})$ direction. Note that both electric and magnetic flux are defined modulo 2 in correspondence with the Z_2 gauge theory. After simple algebra,

$$\begin{aligned} F_y|\xi_{ab}\rangle &= (-1)^a|\xi_{ab}\rangle \\ F_x|\xi_{ab}\rangle &= (-1)^b|\xi_{ab}\rangle \end{aligned} \tag{C2}$$

Compare Eqn. C1 and C2 with Eqn. 23, we arrive at the conclusions listed in Table I.

Appendix D: Modular Transformations

The $\mathcal{S}$ and $\mathcal{U}$ matrices describe the action of modular transformations on the degenerate ground states of the topological quantum field theory on a torus. For Abelian phases, the ij'th entry of the $\mathcal{S}$ matrix corresponds to the phase the i'th quasi-particle acquires when it encircles the j'th quasi-particle. The $\mathcal{U}$ matrix is diagonal and the ii'th entry corresponds to the phase the i'th quasi-particle acquires when it is exchanged with an identical one. Let us first review the geometric meaning of these transformations. Labeling our system by complex coordinates $z = x + iy$, the torus may be defined by the periodicity of ω_1 and ω_2 along the two directions $\hat{e_1}$ and $\hat{e_2}$ (need not to be orthogonal) i.e. $z \equiv z + \omega_1 \equiv z + \omega_2$. Now consider a transformation

$$\begin{pmatrix} \omega_1 \\ \omega_2 \end{pmatrix} \to \begin{pmatrix} \omega_1' \\ \omega_2' \end{pmatrix} = \begin{pmatrix} a & b \\ c & d \end{pmatrix} \begin{pmatrix} \omega_1 \\ \omega_2 \end{pmatrix} \tag{D1}$$

where $a, b, c, d \in \mathbb{Z}$. Since our system lives on a lattice, the inverse of the above matrix should again have integer components, hence the determinant $ad - bc = 1$. One can show that matrices with these properties form a group, called $SL(2, \mathbb{Z})$. Interestingly, all the elements in this group can be obtained by a successive application of the following two generators of $SL(2, \mathbb{Z})$:

- $S = \begin{pmatrix} 0 & 1 \\ -1 & 0 \end{pmatrix}$. This transformation corresponds to $\omega_1 \to \omega_2$ and $\omega_2 \to -\omega_1$ and therefore, for a square geometry corresponds to rotation of the system by 90^o.

- $U = \begin{pmatrix} 1 & 1 \\ 0 & 1 \end{pmatrix}$. Under this transformation $\omega_1 \to \omega_1' = \omega_1 + \omega_2$ and $\omega_2 \to \omega_2' = \omega_2$. Consider a loop on the torus with winding numbers n_1 and n_2 along ω_1 and ω_2 directions. By definition of the U transformation, the winding numbers in the transformed basis:

$$\begin{aligned} & n_1\omega_1 + n_2\omega_2 \\ = \; & n_1(\omega_1' - \omega_2') + n_2\omega_2' \\ = \; & n_1'\omega_1' + n_2'\omega_2' \end{aligned}$$

  where $n_1' = n_1$ and $n_2' = n_2 - n_1$ are the winding numbers along the ω_1' and ω_2' directions.

The transformation properties of the resulting MESs under modular transformations would yield the desired $\mathcal{S}$ and $\mathcal{U}$ matrices. Further, for a symmetry transformation of $F(S, U)$ on $(\omega_1, \omega_2)^T$, the corresponding modular transformation on MESs would yield the modular $\mathcal{F}(\mathcal{S},\mathcal{U})$ matrix.

In the main text, we have obtained $\mathcal{S}$ and $\mathcal{U}$ matrices for the toric code model from the action of these transformations on the basis states $|\xi_{ab}\rangle$. We now show that one can also obtain the $\mathcal{U}\mathcal{S}$ matrix by studying the action of $2\pi/3$ rotation $R_{2\pi/3}$ on the MESs (provided that $R_{2\pi/3}$ is symmetry of the model). To see this, consider a triangular lattice that is defined by two lattice vectors (complex numbers) ω_1, ω_2 with $\omega_1 = (1, 0)$ and $\omega_2 = (1/2, \sqrt{3}/2)$. The transformation of our interest is the transformation of ω_1, ω_2 under $R_{2\pi/3}$ rotation: $\omega_1 \to \omega_1' = -\omega_1 + \omega_2$ and $\omega_2 \to \omega_2' = -\omega_1$. Therefore, one can write the $R_{2\pi/3}$-matrix

$$R_{2\pi/3} = \begin{pmatrix} -1 & 1 \\ -1 & 0 \end{pmatrix} \tag{D2}$$

This matrix belongs to the group $SL(2, \mathbb{Z})$ and simple algebra shows that $R_{2\pi/3} = US$. One may also check that $R_{2\pi/3}^3 = 1$ as one might expect. Therefore, knowing the action of $R_{2\pi/3}$ on the MESs would lead to the $\mathcal{U}\mathcal{S}$ matrix.

Appendix E: Modular matrices of Z_2 gauge theory by transforming minimum entropy states

Let's study the action of modular transformation on the MESs $|\Xi_\alpha\rangle$ for the Z_2 gauge theory in Sec. IV B and compare the resulting modular matrices with the known results.

First consider a $\pi/2$ rotation symmetric square sample. Under $\pi/2$ rotation, $|\xi_{ab}\rangle \to |\xi_{ba}\rangle$. According to Eqn.23, the transformation for the MESs $|\Xi_\alpha\rangle$ for cuts along $\hat{y}$:

$$\begin{aligned} |\Xi_1\rangle &\to \frac{1}{2}\left(|\Xi_1\rangle + |\Xi_2\rangle + |\Xi_3\rangle + |\Xi_4\rangle\right) \\ |\Xi_2\rangle &\to \frac{1}{2}\left(|\Xi_1\rangle + |\Xi_2\rangle - |\Xi_3\rangle - |\Xi_4\rangle\right) \\ |\Xi_3\rangle &\to \frac{1}{2}\left(|\Xi_1\rangle - |\Xi_2\rangle + |\Xi_3\rangle - |\Xi_4\rangle\right) \\ |\Xi_4\rangle &\to \frac{1}{2}\left(|\Xi_1\rangle - |\Xi_2\rangle - |\Xi_3\rangle + |\Xi_4\rangle\right) \end{aligned}$$

Hence, the modular $\mathcal{S}$ matrix is given by

$$\mathcal{S} = \frac{1}{2}\begin{pmatrix} 1 & 1 & 1 & 1 \\ 1 & 1 & -1 & -1 \\ 1 & -1 & 1 & -1 \\ 1 & -1 & -1 & 1 \end{pmatrix}$$

This is exactly what one expects from the topological quantum field theory corresponding to the zero correlation length deconfined-confined Z_2 gauge theory. There are four flavors of quasi-particles in the spectrum: $1, m, e, em$, as we have shown in Table I. The electric charge e and magnetic charge (vison) m both have self-statistics of a boson and pick up a phase of π when they encircle each other (and as a corollary, the same phase when they encircle em). By studying $\mathcal{S}$, one gets the self and mutual statistics for quasi-particles encircling each other.

In Sec III A we further show that symmetry is not required to determine the $\mathcal{S}$ matrix. In Eqn. 23 we have shown the MESs for cuts along $w_2 = \hat{y}$ direction:

$$\begin{aligned} |\Xi_1\rangle &= \frac{e^{i\varphi_1}}{\sqrt{2}}(|\xi_{00}\rangle + |\xi_{01}\rangle) \\ |\Xi_2\rangle &= \frac{e^{i\varphi_2}}{\sqrt{2}}(|\xi_{00}\rangle - |\xi_{01}\rangle) \\ |\Xi_3\rangle &= \frac{e^{i\varphi_3}}{\sqrt{2}}(|\xi_{10}\rangle + |\xi_{11}\rangle) \\ |\Xi_4\rangle &= \frac{e^{i\varphi_4}}{\sqrt{2}}(|\xi_{10}\rangle - |\xi_{11}\rangle) \end{aligned}$$

where φ_i are undetermined phases for MESs $|\Xi_i\rangle$. The unitary matrix U_1 connecting the w_2 MESs and the electric flux states:

$$U_1 = \frac{1}{\sqrt{2}}\begin{pmatrix} e^{i\varphi_1} & e^{i\varphi_2} & & \\ e^{i\varphi_1} & -e^{i\varphi_2} & & \\ & & e^{i\varphi_3} & e^{i\varphi_4} \\ & & e^{i\varphi_3} & -e^{i\varphi_4} \end{pmatrix} \qquad \text{(E1)}$$

On the other hand, it is straightforward to verify that for loops along $w_2' = -\hat{x} + \hat{y}$ direction, which satisfies our requirement Eqn.8, the corresponding MESs:

$$\begin{aligned} |\Xi_1'\rangle &= \frac{e^{i\varphi_1'}}{\sqrt{2}}(|\xi_{00}\rangle + |\xi_{11}\rangle) \\ |\Xi_2'\rangle &= \frac{e^{i\varphi_2'}}{\sqrt{2}}(|\xi_{00}\rangle - |\xi_{11}\rangle) \\ |\Xi_3'\rangle &= \frac{e^{i\varphi_3'}}{\sqrt{2}}(|\xi_{01}\rangle + |\xi_{10}\rangle) \\ |\Xi_4'\rangle &= \frac{e^{i\varphi_4'}}{\sqrt{2}}(|\xi_{01}\rangle - |\xi_{10}\rangle) \end{aligned}$$

again φ_i' are undetermined phases for MESs $|\Xi_i'\rangle$. The unitary matrix U_2 connecting the w_2' MESs and the electric flux states:

$$U_2 = \frac{1}{\sqrt{2}}\begin{pmatrix} e^{i\varphi_1'} & e^{i\varphi_2'} & & \\ & & e^{i\varphi_3'} & e^{i\varphi_4'} \\ & & e^{i\varphi_3'} & -e^{i\varphi_4'} \\ e^{i\varphi_1'} & -e^{i\varphi_2'} & & \end{pmatrix} \qquad \text{(E2)}$$

Combining Eqn. E1 and E2, we can write down the modular $\mathcal{S}$ matrix as:

$$\begin{aligned} \mathcal{S} &= U_2^{-1}U_1 \\ &= \frac{1}{2}\begin{pmatrix} e^{i(\varphi_1-\varphi_1')} & e^{i(\varphi_2-\varphi_1')} & e^{i(\varphi_3-\varphi_1')} & -e^{i(\varphi_4-\varphi_1')} \\ e^{i(\varphi_1-\varphi_2')} & e^{i(\varphi_2-\varphi_2')} & -e^{i(\varphi_3-\varphi_2')} & e^{i(\varphi_4-\varphi_2')} \\ e^{i(\varphi_1-\varphi_3')} & -e^{i(\varphi_2-\varphi_3')} & e^{i(\varphi_3-\varphi_3')} & e^{i(\varphi_4-\varphi_3')} \\ e^{i(\varphi_1-\varphi_4')} & -e^{i(\varphi_2-\varphi_4')} & -e^{i(\varphi_3-\varphi_4')} & -e^{i(\varphi_4-\varphi_4')} \end{pmatrix} \end{aligned}$$

To ensure the existence of an identity particle in accord with the first row and column, we impose the conditions:

$$\begin{aligned} &\varphi_1' = \varphi_2' = \varphi_3' = \varphi_4' \\ =\ &\varphi_1 = \varphi_2 = \varphi_3 = \varphi_4 + \pi \end{aligned}$$

This leads to the following modular $\mathcal{S}$ matrix:

$$\mathcal{S} = \frac{1}{2}\begin{pmatrix} 1 & 1 & 1 & 1 \\ 1 & 1 & -1 & -1 \\ 1 & -1 & 1 & -1 \\ 1 & -1 & -1 & 1 \end{pmatrix}$$

which is indeed the correct result for Z_2 toric code.

Now consider the transformation corresponding to $\mathcal{U}$ matrix as described in Appendix D, where $n_1' = n_1$ and $n_2' = n_2 - n_1$ are the winding numbers along the ω_1' and ω_2' directions. Using this expression and Eqn.23, the transformation for MESs from w_2 cut to w_2' cut:

$$\begin{aligned} |\Xi_1\rangle &\rightarrow |\Xi_1\rangle \\ |\Xi_2\rangle &\rightarrow |\Xi_2\rangle \\ |\Xi_3\rangle &\rightarrow |\Xi_3\rangle \\ |\Xi_4\rangle &\rightarrow -|\Xi_4\rangle \end{aligned}$$

This leads to the following modular $\mathcal{U}$ matrix:

$$\mathcal{U} = \begin{pmatrix} 1 & 0 & 0 & 0 \\ 0 & 1 & 0 & 0 \\ 0 & 0 & 1 & 0 \\ 0 & 0 & 0 & -1 \end{pmatrix}$$

Again, this is what is expected from the Z_2 gauge theory. The sign of -1 on the last entry of the diagonal corresponds to the fermionic self statistics of the em while the positive signs correspond to the bosonic self statistics of $1, e$ and m particles.

To see a more generic example to derive the $\mathcal{U}$ matrix from rotation symmetry, we first define the toric code on a triangular lattice, with system dimensions such that the $2\pi/3$ rotation is a symmetry of the system. The Hamiltonian is same as Eq. 15 with the star 's' denoting six links emanating from a vertex while the plaquette 'p' now involves three links. We again denote the four degenerate ground states on a torus as $|\xi_{ab}\rangle$ with $a, b = 0, 1$ denoting the parity of electric field along the non-contractible cycles. The relation between the MESs $|\Xi_\alpha\rangle$ and the states $|\xi_{ab}\rangle$ remains unchanged (Eqn. 23). The calculation for the transformation under $2\pi/3$ proceeds analogously to that for $\pi/2$ rotation and one finds:

$$\begin{aligned} R_{2\pi/3}|\xi_{00}\rangle &= |\xi_{00}\rangle \\ R_{2\pi/3}|\xi_{01}\rangle &= |\xi_{10}\rangle \\ R_{2\pi/3}|\xi_{10}\rangle &= |\xi_{11}\rangle \\ R_{2\pi/3}|\xi_{11}\rangle &= |\xi_{01}\rangle \end{aligned}$$

Translating the action of $R_{2\pi/3}$ on the states $|\xi_\alpha\rangle$ to that on states $|\Xi_\alpha\rangle$, one finds

$$\mathcal{US} = \frac{1}{2}\begin{pmatrix} 1 & 1 & 1 & 1 \\ 1 & 1 & -1 & -1 \\ 1 & -1 & 1 & -1 \\ -1 & 1 & 1 & -1 \end{pmatrix}$$

Combining the expression and the $\mathcal{S}$ matrix, one obtains

$$\mathcal{U} = \begin{pmatrix} 1 & 0 & 0 & 0 \\ 0 & 1 & 0 & 0 \\ 0 & 0 & 1 & 0 \\ 0 & 0 & 0 & -1 \end{pmatrix}$$

as expected.

[1] Xiao-Gang Wen, *Quantum field theory of many-body systems*, Oxford Graduate Texts, 2004.
[2] P.W. Anderson, Science 237, 1196 (1987).
[3] X.-G. Wen, Int. J. Mod. Phys. B4, 239 (1990).
[4] N. Read and B. Chakraborty, Phys. Rev. B 40, 7133 (1989).
[5] X.-G. Wen, Phys. Rev. B 44, 2664 (1991).
[6] N. Read and S. Sachdev, Phys. Rev. Lett. 66, 1773 (1991); S. Sachdev, Physical Review B 45, 12377 (1992).
[7] T. Senthil and M. P. A. Fisher. Phys. Rev. B 62, 7850 (2000).
[8] R. Moessner and S. L. Sondhi, Phys. Rev. Lett. 86, 1881 (2001).
[9] P. A. Lee, Rep. Prog. Phys. 71, 012501 (2008).
[10] L. Balents, Nature 464, 199 (2010).
[11] A. Kitaev, Ann. Phys., 303, 2 (2003).
[12] see e.g. Chetan Nayak, Steven H. Simon, Ady Stern, Michael Freedman, and Sankar Das Sarma, Rev. Mod. Phys. 80, 1083 (2008).
[13] A. Hamma, R. Ionicioiu, and P. Zanardi, Phys. Lett. A 337, 22 (2005); Phys. Rev. A 71, 022315 (2005).
[14] M. Levin, X.-G. Wen, Phys. Rev. Lett. 96, 110405 (2006).
[15] A. Kitaev, J. Preskill, Phys. Rev. Lett. 96, 110404 (2006).
[16] E. Keski-Vakkuri and Xiao-Gang Wen, Int. J. Mod. Phys. B7, 4227 (1993).
[17] P. Di Francesco, P. Mathieu, D. Senechal, *Conformal field theory,* Springer 1997.
[18] A. Kitaev Ann. Phys. 321, 2 (2006).
[19] Erik P. Verlinde, Nucl. Phys. B300:360, (1988).
[20] F.A. Bais, J.C. Romers, arXiv:1108.0683v1.
[21] V. Kalmeyer and R. B. Laughlin, Phys. Rev. Lett. 59, 2095; V. Kalmeyer and R. B. Laughlin, Phys. Rev. B 39, 11 879; X. G. Wen, Frank Wilczek, and A. Zee, Phys. Rev. B 39, 11 413 (1989).
[22] Shiying Dong, Eduardo Fradkin, Robert G. Leigh, Sean Nowling, JHEP 0805:016(2008).
[23] S. Yan, D. A. Huse, S. R. White, Science 332, 1173 (2011).
[24] H.-C. Jiang, Z. Y. Weng, D. N. Sheng, Phys. Rev. Lett. 101, 117203 (2008).
[25] Z. Y. Meng, T. C. Lang, S. Wessel, F. F. Assaad, A. Muramatsu, Nature 464, 847 (2010).
[26] H.-C. Jiang, H. Yao, L. Balents, arXiv:1112.2241.
[27] L. Wang, Z.-C. Gu, F. Verstraete, X.-G. Wen, arXiv:1112.3331.
[28] D. N. Sheng, Z. C. Gu, K. Sun, and L. Sheng, Nature Commun. 2, 389 (2011).
[29] E. Tang, J. W. Mei, and X. G. Wen, Phys. Rev. Lett. 106, 236802 (2011).
[30] T. Neupert, L. Santos, C. Chamon, and C. Mudry, Phys. Rev. Lett. 106, 236804 (2011).
[31] Yi-Fei Wang, Hong Yao , Zheng-Cheng Gu , Chang-De Gong, D. N. Sheng, Phys. Rev. Lett. 108, 126805 (2012).
[32] N. Regnault and B. A. Bernevig, Phys. Rev. X 1, 021014 (2011).
[33] Yi Zhang, Tarun Grover, Ashvin Vishwanath, Phys. Rev. Lett. 107, 067202 (2011); Yi Zhang, Tarun Grover, Ashvin Vishwanath, Phys. Rev. B 84, 075128 (2011).
[34] S. Furukawa and G. Misguich, Phys. Rev. B 75, 214407 (2007).
[35] Masudul Haque, Oleksandr Zozulya, and Kareljan Schoutens Phys. Rev. Lett. 98, 060401 (2007); O. S.

Zozulya, M. Haque, K. Schoutens, and E. H. Rezayi, Phys. Rev. B 76, 125310 (2007).
[36] Hong Yao and Xiao-Liang Qi, Phys. Rev. Lett. 105, 080501 (2010).
[37] Sergei V. Isakov, Matthew B. Hastings, Roger G. Melko, Nature Physics 7, 772 (2011).
[38] Hui Li and F. D. M. Haldane , Phys. Rev. Lett. 101, 010504 (2008).
[39] Michael A. Levin and Xiao-Gang Wen, Phys RevB. 71.045110 (2005).
[40] C. Gros, Ann. Phys. 189, 53 (1989).
[41] M. B. Hastings et al., Phys. Rev. Lett. 104, 157201(2010).
[42] S. T. Flammia et al, Phys. Rev. Lett. 103, 261601 (2009).
[43] M.A. Nielsen and I.L. Chuang, *Quantum Computation and Quantum Information*, (Cambridge University Press, 2000).
[44] D. F. Schroeter, E. Kapit, R. Thomale, and M. Greiter, Phys. Rev. Lett. 99, 097202 (2007).
[45] C. Castelnovo, C. Chamon, Phys. Rev. B 78, 155120 (2008).
[46] T. Grover, A. Turner and A. Vishwanath, Phys. Rev. B 84, 075128 (2011).